20. A. I. Funtikov, "A method of studying phase transitions at high pressures using shock compression of porous materials," FGV, 5, No. 4 (1969).
21. K. K. Krupnikov, M. I. Brazhnik, and V. P. Krupnikova, "Shock compression of porous tungsten," Zh. Eksp. Teor. Fiz. 42, No. 3 (1962).
22. V. F. Anisichkin, "Generalized shock adiabatic curves of elements," Zh. Prikl. Mekh. Tekh. Fiz. No. 3 (1978).

RESISTANCE OF ALUMINUM AD-1 AND DURALUMINUM D-16 TO PLASTIC DEFORMATION UNDER SHOCK COMPRESSION CONDITIONS

A. N. Dremin, G. I. Kanel', and O. B. Chernikova

UDC 532.593

It is known that the strength properties of a material affect the nature of the evolution and the damping rate therein of shocks of tens of gigapascals in amplitude sufficiently substantially [1-3]. Recording of the evolution of a one-dimensional compression pulse permits determination of the trajectories of the change in state of fixed specimen particles in the coordinates: stress σ_x in the compression direction-specific volume V [4]. Then from the divergence between the trajectories of the change in state and the multilateral compression curve p(V) (for instance, the equilibrium isentropy), by taking account of the one-dimensionality of the total deformation, a law for the variation of the shear stress during deformation can be found and the resistance to deformation can thereby be determined at different stages of compression pulse passage through the specimen particle being checked. Such measurements are performed in this paper for technical aluminum AD-1 with the density 2.71 g/cm³ and duraluminum D-16 with the density 2.78 g/cm³ for two compression pulse amplitudes.

The diagram for the tests is shown in Fig. 1. A one-dimensional compression pulse of initially rectangular shape is generated in the specimen 1 by the impact of an aluminum plate (impactor) 2 accelerated by using an explosive apparatus. Two series of tests are executed, in the first of which the impactor thickness is δ = 5 mm and its velocity is W = 595 ± 10 m/sec. and in the second δ = 4 mm, and W = 1505 ± 20 m/sec. The diameter of the flat section of the impactor was 55-65 mm at the time of collision. The compression pulse was recorded by using manganin pressure transducers 3 located 4-15 mm from the collision surface in the specimens. The specimen plates were fabricated from 120-mm diameter circular billets in the delivered state. The transducers had the area ∿5 × 5 mm, the thickness 0.03 mm, and initial resistance ∿3.5 Ω, and were separated from the specimen surface by 0.02-mm thick (in the first series) or 0.04-mm thick (in the second series) insulating lavsan films 4 on both sides. During the multiple reflections, the pressure in the low-strength insulation is set equal to the normal stress in the compression direction σ_x. Here and henceforth we shall take the compressive stress positive. The stress profiles $\sigma_x(t)$ for aluminum obtained from processing experimental data, are presented in Fig. 2; the stress profiles $\sigma_x(t)$ for duraluminum differ insignificantly. The distance from the collision surface to the transducer is shown in millimeters by the number on the curves. Each curve is obtained by taking the average of the results of at least two measurements, where the hysteresis in the readings of the manganin pressure transducers [5] was taken into account in the processing. According to the test conditions, the rear impactor surface in the second series was in contact with paraffin, consequently, the unloading was not traced completely in these tests.

The elastic part of the rarefaction wave is isolated sufficiently clearly on the pressure profiles. The transition from elastic to plastic waves is smooth and blurred. The tightened "tail" of the rarefaction wave is fixed in the first series of tests. The elastic predecessor of the compression was not determined clearly by the manganin transucers in either the aluminum or the duraluminum case. The characteristic time for shock front growth was ∿0.08-0.11 μsec on the oscillograms for the first test series, and ∿0.05-0.08 μsec for the second test series.

Chernogolovka. Translated from Zhurnal Prikladnoi Mekhaniki i Tekhnicheskoi Fiziki, No. 4, pp. 132-138, July-August, 1981. Original article submitted May 30, 1980.

 0021-8944/81/2204-0558$07.50 © 1982 Plenum Publishing Corporation

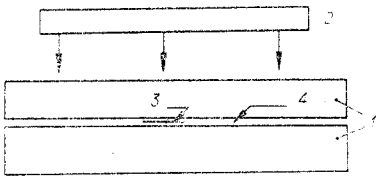

Fig. 1

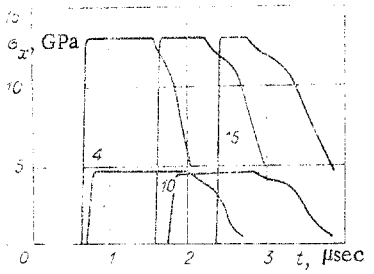

Fig. 2

It is evident that since an interlayer of material with a lower dynamic stiffness is inserted in the specimen for recording, there is a certain inertia and hence, the profiles $\sigma_x(t)$ are recorded with some distortion. To estimate the influence of the distortions induced by the transducer insulation on the recorded profile $\sigma_x(t)$ in the specimen, the collision of two plates of elastic-plastic material (aluminum) was modeled numerically, where one of the plates (the specimen) contained two interlayers of liquidy material. The system of gasdynamic equations, including the equation of motion, the continuity equation, and the equation of state, was solved by a through method using a "checkerboard" computational mesh and quadratic pseudoviscosity [6]. The equation of state for the global stress and strain tensor components was given in the form

$$p(V) = \left\{\exp\left(4b\frac{V_0 - V}{V_0}\right) - 1\right\}\rho_0 c_0^2/4b, \tag{1}$$

where p is the pressure; V_0, V are the initial and running specific volumes; $\rho_0 = 1/V_0$ is the initial density; c_0, b are coefficients in the linear relation between the shock velocity D and the jump in the mass flow rate in the wave u ($D = c_0 + bu$). Equation (1) is obtained by integrating the expression for the speed of sound [7] under the assumption of agreement between the shock adiabat and the unloading isentrope in a one-dimensional simple wave in p–u coordinates. The quantities c_0, b, and ρ_0 were taken equal to $5.34 \cdot 10^5$ cm/sec, and 1.36 and 2.71 g/cm^3, respectively. Since the pressure jump in the shock, and therefore, the irreversible heating of the material for the case being computed were comparatively small, the energy conservation equation was not taken into account in the computation and the temperature was not computed.

The deviator component of the stress tensor for the one-dimensional strain case under consideration is characterized by the stresses [1]

$$\sigma_x - p = \frac{4}{3}\sigma_{xy}, \quad \sigma_y - p = \sigma_z - p = -\frac{2}{3}\sigma_{xy}, \quad \sigma_{xy} = \sigma_{xz}, \quad \sigma_{yz} = 0.$$

The relation between the shear stress increments $d\sigma_{xy}$ and the maximal shear strain $d\varepsilon_{xy}$ is given in the form

$$d\sigma_{xy} = \begin{cases} G d\varepsilon_{xy}, & \text{if} \quad |\sigma_{xy}| < \sigma_T/2, \\ 0, & \text{if} \quad |\sigma_{xy}| = \sigma_T/2, \end{cases}$$
$$d\varepsilon_{xy} = d\varepsilon_x - d\varepsilon_y = -dV/V,$$

where G is the shear modulus, σ_T is the yield for the case of a uniaxial stress state, ε_x, ε_y are the total strains in the longitudinal and transverse directions, where $d\varepsilon_x = -dV/V$, $d\varepsilon_y = 0$. The dependence of the aluminum shear modulus on the pressure was taken from [7], and the dependence of the yield on the pressure was given arbitrarily in the form

$$\sigma_T = 2 \cdot 10^9 \frac{\text{dyne}}{\text{cm}^2} + 0.01p.$$

Results of computing the profiles $\sigma_x(t)$ in specimens without interlayers as well as the pressure profiles in the middle sections of fluoroplastic interlayers 0.1-mm thick are presented in Fig. 3 (the coordinates of the sections being checked are kept the same). The solid lines depict the profiles $\sigma_x(t)$ in the specimen without interlayers, the dash–dot lines depict the pressure profiles at the center of the interlayer in the case of a specimen with one interlayer, and the dashes do the same in the case of a specimen with two interlayers

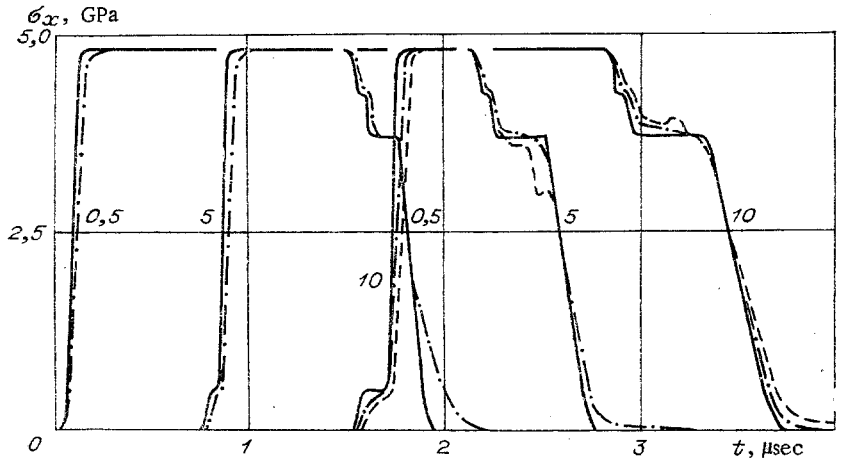

Fig. 3

(simultaneous recording by two transducers located at different coordinates). The numbers display the distance in millimeters from the collision surface. The spatial spacing in the computation was 0.025 mm, and the time spacing was 0.5 nsec.

Results of the computations show that the introduction of insulating interlayers in the specimens actually yields distortion of the stress profiles being recorded, and all the more the more the dynamic stiffnesses of the specimen and the insulating interlayers differ. In the case of two transducers, cumulative distortion is observed on the p(t) profile in the second interlayer; a short rarefaction pulse, appearing as a result of shock reflection from the second interlayer in the specimen, is imposed on the profile p(t) for the first interlayer. In the case of one transducer (a specimen with one interlayer) the distortions are systematic in nature; the lag in the profile p(t) at the center of the interlayer with respect to the profile $\sigma_x(t)$ at the same coordinate in a specimen without interlayers is practically independent of the distance transversed by the wave. In case the interlayer is placed in the specimen directly close (0.5 mm) to the collision surface, anomalous distortion of the "tail" part of the rarefaction wave is observed, which is a result of superposition of the rarefaction pulse reflected from the rear surface of the impactor, that appears during shock passage through the interlayer. For a large distance between the interlayer and the collision surface this pulse being superposed is shifted relative to the main pulse with an increase in the lag time.

Therefore, the results of model computations show that the distortions induced by the insulations actually being used are negligible and of systematic nature for recordings of the profile $\sigma_x(t)$ by one transducer (or several transducers but arranged in one section of the specimen) at a sufficient distance from the collision surface. This permits utilization of the simple wave approximation for the construction of the trajectories of the change of state, according to which the change in the volume dV is computed as

$$dV = d\sigma_x/\rho_0^2 a^2(\sigma_x), \tag{2}$$

where a is the velocity of propagation of one wave element in Lagrangean coordinates, i.e., in a coordinate system coupled to the specimen. It has been shown by numerous experiments [2, 3, 8-10] that under shock loading conditions the viscoelastic properties of the medium are governing. Hence, the connection between the resistance to deformation and the velocity of plastic deformation was sought in this paper. To this end, the total shear strain ε_{xy} was separated into elastic and plastic components; then the velocity of plastic shear strain is

$$\dot{\varepsilon}_{xy}^{pl} = \dot{\varepsilon}_{xy} - \dot{\varepsilon}_{xy}^{el} = -\frac{\dot{V}}{V} - \frac{\dot{\sigma}_{xy}}{G}; \tag{3}$$

$$\dot{\sigma}_{xy} = \frac{3}{4}\dot{\sigma}_x\left(1 - a_V^2/a^2\right), \tag{4}$$

where a_V is the volume speed of sound in Lagrange coordinates, determined from (1).

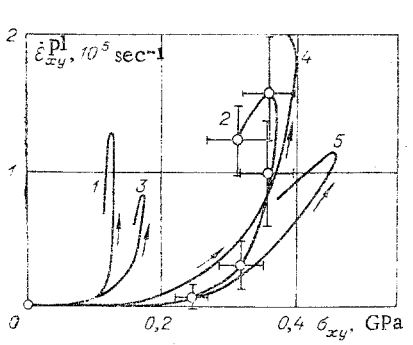

Fig. 4

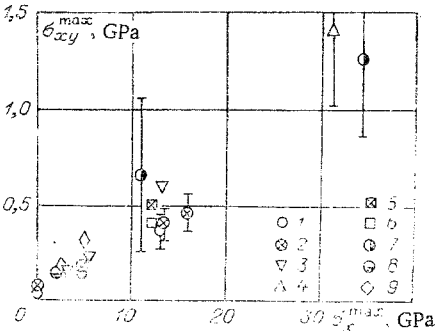

Fig. 5

The magnitude of the maximum shear stress σ_{xy} was determined by integrating (4). Such a computation is performed only for the rarefaction wave, where a point on the shock adiabat for $\sigma_{xy} = 0$ is taken as the initial state for the trajectories of the change of state (2) and the multilateral compression curve (1).

The dependences $\dot{\varepsilon}^{pl}_{xy}(\sigma_{xy})$ obtained as a result of processing the experimental data for aluminum (curves 1 and 2) and duraluminum (curves 3 and 4) are presented in Fig. 4 (curve 5 is constructed from the results of measurements [8]). The maximum stress σ_x in the compression pulse was 4.7-4.8 GPa in the first series of tests (curves 1 and 3), and 13.1-13.4 GPa in the second series (curves 2 and 4). Curve 5 is constructed from the results of tests with a shock of 16.0 GPa amplitude. All the graphs are constructed for unloading to 20-30% of the amplitude value of σ_x. The error, estimated by the spread in the experimental data, in constructing the graph of $\dot{\varepsilon}^{pl}_{xy}(\sigma_{xy})$ is displayed in curve 2.

The graphs presented in Fig. 4 graphically demonstrate the dependence of the resistance to plastic deformation on the amplitude of the compression pulse. Judging by the shape of the curves $\dot{\varepsilon}^{pl}_{xy}(\sigma_{xy})$, a change in the magnitude of the shear stress in the rarefaction wave is only partially reversible, which indicates the substantial contribution of hardening to the dependence of the resistance to plastic deformation on the amplitude of the compression pulse. Comparison of the results for aluminum AD-1 and duraluminum D-16 shows that the difference in the strength properties of these materials, which is perceptible at low amplitudes, is practically equilibrated with the growth in compression pulse intensity.

It is seen from Fig. 4 that the dependences $\dot{\varepsilon}^{pl}_{xy}(\sigma_{xy})$ are substantially nonlinear, where this nonlinearity is strongest for the case of a low intensity compression pulse in aluminum (curve 1). Judging by the nature of the recorded profiles $\sigma_x(t)$ and the dependences $\dot{\varepsilon}^{pl}_{xy}(\sigma_{xy})$, the behavior of aluminum alloys in a shock could be described by the model of an ideal elastic-plastic body with a yield point dependent on the acting pressure. However, such a description contradicts the results of recording the wave evolution under step loading of aluminum alloys [8, 9], from which it follows that upon "pressing" of a shock-compressed material by a second wave it will behave almost the same as under unloading, its reaction in the initial stage corresponding mainly to pure elastic deformation. Evidently such behavior of the material is due to superposition of two processes, multiplication of the "plastic deformation carriers" (not only dislocations) under the effect of shear stresses, and their being blocked, and annihilated with time.

The maximum values of the shear stresses σ^{max}_{xy} for aluminum alloys are compared with data in the literature in Fig. 5 as a function of the compression pulse amplitude σ^{max}_{x}. The points 1 and 2 describe data for AD-1 and D-16, respectively; the points 3 are obtained in [3] for the alloy 2024 (an analog of D-16) by a method close to that used in this paper; 4 in [11] (the alloy 2024); 5 and 6 in [12] (for the alloys 2024, and 1060, respectively); 7 in [13] by studying the damping of shock waves; the points 8 in [14] (the alloy 6061-T6) are obtained from an analysis of the rarefaction wave structure, and the "preload" compression wave for the step loading. Here results of measuring the resistance to shear are presented as a function of the pressure under static conditions, the points 9 from [15]. The data presented in Fig. 5 afford a foundation for the following deductions. The resistance to plastic deformation at elevated pressures is somewhat lower under shock compression conditions than under static conditions. Recording of the shock attenuation is associated with great error in the determination of the resistance to plastic deformation, and results in elevated values as compared with the direct recording of the profile $\sigma_x(t)$. The difference

in the resistance of different alloys to plastic deformation as the shock compression pressure grows is equilibrated, the difference in the quantities σ_{xy}^{max} characterizing the alloy properties under normal conditions is conserved, but the ratio of these quantities is not conserved in every case. In a first approximation the dependence of the magnitude of the resistance to shear deformation on the shock compression pressure can be described by the linear relationship.

$$\sigma_{xy}^{max}(p) = \sigma_{xy}^{0} + K\sigma_{x}^{max},$$

where σ_x^0 = 0.08 ± 0.05 GPa and K = 0.030 ± 0.006.

The authors are grateful to G. A. Savel'ev for aid in preparing and performing the measurements.

LITERATURE CITED

1. L. V. Al'tshuler, M. I. Brazhnik, and G. S. Telegin, "Strength and elasticity of iron and copper at high shock compression pressures," Prikl. Mekh. Tekh. Fiz., No. 6 (1971).
2. P. G. A. Fuller and J. H. Price, "Dynamic stress-strain release path for aluminum and magnesium to 200 kbar," Brit. J. Appl. Phys., Ser. 2, J. Phys. D, No. 2 (1969).
3. A. S. Kusubov and M. Thiel, Measurements of elastic and plastic unloading wave profiles in 2024-T4 aluminum alloy," J. Appl. Phys., 40, No. 9 (1969).
4. G. I. Kanel', "On the experimental determination of the kinetics of relaxation processes under shock compression of condensed media," Prikl. Mekh. Tekh. Fiz., No. 5 (1977).
5. G. I. Kanel', G. G. Vakhitova, and A. N. Dremin," Metrological characteristics of manganin pressure transducers under shock compression and unloading conditions," Fiz. Goren. Vykhryva, No. 2 (1978).
6. A. A. Samarskii and Yu. P. Popov, Difference Schemes of Gasdynamics [in Russian], Nauka, Moscow (1975).
7. A. A. Vorob'ev, A. N. Dremin, and G. I. Kanel', "Dependence of the aluminum elasticity coefficients on the degree of compression in a shock," Prikl. Mekh. Tekh. Fiz., No. 5 (1974).
8. A. N. Dremin and G. I. Kanel', "Compression and rarefaction waves in shock-compressed metals," Prikl. Mekh. Tekh. Fiz., No. 2 (1976).
9. J. Lipkin and J. R. Asay, "Reshock and release of shock-compressed 6061-T6 aluminum," J. Appl. Phys., 48, No. 1 (1977).
10. G. I. Kanel', "Viscoelastic properties of metals in a shock wave," in: Detonation. Critical Phenomena. Physicochemical Transformations in Shocks [in Russian], Chernogolovka (1978).
11. A. S. Kusubov and M. Thiel, "Dynamic yield strength of 2024-T4 aluminum at 313 kbar," J. Appl. Phys. 40, No. 2 (1969).
12. J. O. Erkman, "Elastoplastic effects in the attenuation of shock waves," in: Proc. 4th Internat. Sympos. on Detonation, 277, Washington (1967).
13. J. O. Erkman and J. Christensen, "Attenuation of shock waves in aluminum," J. Appl. Phys. 38, No. 13 (1967).
14. J. R. Asay and J. Lipkin, "A self-consistent technique for estimating the dynamic yield strength of a shock-loaded material," J. Appl. Phys., 49, No. 7 (1978).
15. P. W. Bridgman, Studies in Large Plastic Flow and Fracture, McGraw-Hill, London–New York (1952).